Electronic Supplementary Material (ESI) for Physical Chemistry Chemical Physics.
This journal is © the Owner Societies 2022

Bipolar 1,8-naphthalimides showing high electron mobility and red AIE-active TADF for OLED applications

Naveen Masimukku,[a] Dalius Gudeika,[a] Dmytro Volyniuk,[a] Oleksandr Bezvikonnyi,[a] Jurate Simokaitiene,[a] Vitaly Matulis,[b] Dmitry Lyakhov,[c] Volodymyr Azovskyi,[d] Juozas Vidas Gražulevičius a*

[a] *Kaunas University of Technology, Department of Polymer Chemistry and Technology, K. Baršausko g. 59, LT51423, Kaunas, Lithuania; e-mail: juozas.grazulevicius@ktu.lt*

[b] *Belarusian State University, 4, Nezavisimosti avenue, 220030, Minsk, Republic of Belarus*

[c] *Computer, Electrical and Mathematical Science and Engineering Division, 4700 King Abdullah University of Science and Technology, Thuwal 23955-6900, Saudi Arabia*

[d] *Faculty of Physics, Taras Shevchenko National University of Kyiv, 64/13 Volodymyrs'ka Str., 01601 Kyiv, Ukraine*

Supporting Information

Materials and methods

10*H*-Phenoxazine, tri-*tert*-butylphosphine solution (1.0 M in toluene), palladium(II) acetate, sodium *tert*-butoxide were purchased from Sigma Aldrich. 4-Bromo-*N*-(2-ethylhexyl)-1,8-naphthalimide (**IMBr**), 3,7-di-*tert*-butyl-10*H*-phenothiazine and 2,7-di-*tert*-butyl-9,9-dimethyl-9,10-dihydroacridine were synthesized according to reported literature procedures [1–3].

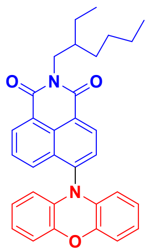

2-(2-Ethylhexyl)-6-(10*H*-phenoxazin-10-yl)-1*H*-benzo[*de*]isoquinoline-1,3(2*H*)-dione (1). 4-Bromo-*N*-(2-ethylhexyl)-1,8-naphthalimide (**IMBr**) (0.5 g, 1.3 mmol), 10*H*-phenoxazine (0.29 g, 1.6 mmol), palladium(II) acetate (0.006 g, 0.027 mmol), tri-*tert*-butylphosphine solution (1.0 M in toluene) (0.032 g, 0.158 mmol), sodium *tert*-butoxide (0.31 g, 3.23 mmol) were dissolved in 15 ml of toluene and heated at 120 °C for 24 h under nitrogen atmosphere. When the reaction was completed, the reaction mixture was diluted with ethylacetete. The product was purified by column chromatography (eluent – *n*-hexane/ethylacetate, 10:1), crystallized from the mixture of *n*-hexane and ethylacetate to get **1** as red crystals. FW = 490.60 g/mol; (yield 0.35 g, 57%); m. p. 176-177 °C. ^{1}H NMR (400 MHz, $CDCl_3$) δ = 8.71 (d, J = 7.7 Hz, 1H), 8.58 (d, J = 7.7 Hz, 1H), 8.35 (d, J = 8.4 Hz, 1H), 7.77 (d, J = 7.7 Hz, 1H), 7.66 (t, J = 7.9 Hz, 1H), 6.71 (d, J = 7.9 Hz, 2H), 6.62 (t, J = 7.7 Hz, 2H), 6.44 (t, J = 7.7 Hz, 2H), 5.62 (d, J = 8.4 Hz, 2H), 4.17 – 4.00 (m, 2H), 1.96 – 1.83 (m, 1H), 1.42 – 1.20 (m, 8H), 0.94 – 0.76 (m, 6H). ^{13}C NMR (101 MHz, $CDCl_3$) δ = 164.2, 163.8, 143.8, 141.5, 133.7, 132.5, 132.1, 130.4, 130.2, 129.6, 128.1, 123.8, 123.5, 123.2, 122.2, 115.9, 113.4, 44.3, 38.0, 30.7, 28.7, 24.0, 23.1, 14.1, 10.6. IR, (KBr), cm^{-1}: 3067 ($CH_{Aromatic}$), 2957, 2926, 2867 ($CH_{Aliphatic}$), 1698 ($C{=}O_{imide}$), 1660, 1618, 1584, 1486 ($C{=}C_{Aromatic}$), 1353, 1334, 1291, 1268 (C-N), 1092, 1065, 1025 (C-O-C), 784, 758, 729, 673 ($CH_{Aromatic}$). MS (APCI$^+$, 20 V), m/z: 491 ([M+H]$^+$). Elemental analysis calcd (%) for $C_{32}H_{30}H_2O_3$: C, 78.34; H, 6.16; N, 5.71; O, 9.78. Found: C, 78.31; H, 6.14; N, 5.72.

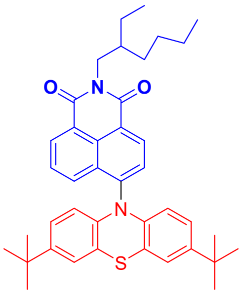

6-(3,7-Di-*tert*-butyl-10*H*-phenothiazin-10-yl)-2-(2-ethylhexyl)-1*H*-benzo[*de*]isoquinoline-1,3(2*H*)-dione (2). Following the synthetic procedure used for the synthesis of derivative **1**, compound **2** was obtained using 3,7-di-*tert*-butyl-10*H*-phenothiazine (0.29 g, 0.92 mmol) instead of 10*H*-phenoxazine. The product was purified by column chromatography (eluent – *n*-hexane/ethylacetate, 10:1), crystallized from the mixture of *n*-hexane and ethylacetate to get **2** as orange crystals. FW = 618.88 g/mol; Yield: 0.24 g, 56%; m. p. 170-171 °C. ^{1}H NMR (400 MHz, CDCl$_3$) δ = 8.72 (d, *J* = 7.7 Hz, 1H), 8.56 (d, *J* = 7.7 Hz, 1H), 8.45 (d, *J* = 8.6 Hz, 1H), 7.84 (d, *J* = 7.7 Hz, 1H), 7.64 (t, *J* = 7.7 Hz, 1H), 7.03 (d, *J* = 2.0 Hz, 2H), 6.68 (dd, J_1 = 8.6 Hz, J_2 = 2.0 Hz, 2H), 5.90 (d, *J* = 8.6 Hz, 2H), 4.19 – 3.99 (m, 2H), 1.99 – 1.85 (m, 1H), 1.43 – 1.20 (m, 8H), 1.14 (s, 18H), 0.94 – 0.75 (m, 6H). ^{13}C NMR (101 MHz, CDCl$_3$) δ = 164.3, 163.9, 146.1, 143.6, 141.1, 132.1, 131.9, 131.1, 130.5, 130.2, 128.0, 124.0, 123.8, 122.9, 119.8, 115.2, 44.3, 38.0, 34.0, 31.1, 30.7, 28.7, 24.0, 23.1, 14.1, 10.6. IR, (KBr), cm^{-1}: 3067 (CH$_{\text{Aromatic}}$), 2958, 2926, 2860 (CH$_{\text{Aliphatic}}$), 1703 (C=O$_{\text{imide}}$), 1656, 1619, 1589, 1478 (C=C$_{\text{Aromatic}}$), 1387, 1357, 1269, 1180 (C-N), 809, 788, 773, 751 (CH$_{\text{Aromatic}}$), 709, 673, 614 (C-S-C). MS (APCI$^+$, 20 V), m/z: 620 ([M+H]$^+$). Elemental analysis calcd (%) for $C_{40}H_{46}N_2O_2S$: C, 77.63; H, 7.49; N, 4.53; O, 5.17, S, 5.18. Found: C, 77.67; H, 7.53; N, 4.56.

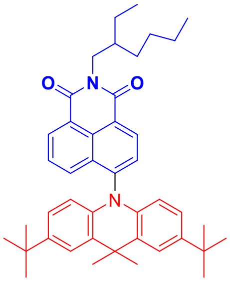

6-(2,7-Di-*tert*-butyl-9,9-dimethylacridin-10(9*H*)-yl)-2-(2-ethylhexyl)-1*H*-benzo[*de*]isoquinoline-1,3(2*H*)-dione (3). Following the synthetic procedure used for the synthesis of derivative **1**, compound **3** was obtained using 2,7-di-*tert*-butyl-9,9-dimethyl-9,10-dihydroacridine (0.4 g, 0.12 mmol) instead of 10*H*-phenoxazine. The product was purified by column chromatography (eluent – *n*-hexane/ethylacetate, 10:1), crystallized from the mixture of *n*-hexane and ethylacetate to get **3** as orange crystals. FW = 628.90 g/mol; Yield: 0.32 g, 50%; m. p. 176-177 °C. ^{1}H NMR (400 MHz, $CDCl_3$) δ = 8.71 (d, J = 7.7 Hz, 1H), 8.56 (d, J = 7.7 Hz, 1H), 8.02 (d, J = 8.6 Hz, 1H), 7.69 (d, J = 7.7 Hz, 1H), 7.56 (t, J = 7.7 Hz, 1H), 7.46 (d, J = 2.0 Hz, 2H), 6.78 (dd, J_1 = 8.6 Hz, J_2 = 2.0 Hz, 2H), 5.79 (d, J = 8.6 Hz, 2H), 4.18 – 4.03 (m, 2H), 2.01 – 1.87 (m, 1H), 1.75 (d, J = 18.5 Hz, 6H), 1.42 – 1.24 (m, 8H), 1.21 (s, 18H), 0.97 – 0.77 (m, 6H). ^{13}C NMR (101 MHz, $CDCl_3$) δ = 164.4, 164.1, 144.7, 143.4, 138.0, 132.6, 131.9, 130.7, 129.3, 127.8, 123.7, 123.4, 122.7, 113.4, 44.3, 38.0, 36.4, 34.2, 32.5, 31.4, 30.7, 28.7, 24.0, 23.1, 14.1, 10.6. IR, (KBr), cm^{-1}: 3067 ($CH_{Aromatic}$), 2957, 2926, 2859 ($CH_{Aliphatic}$), 1699 ($C{=}O_{imide}$), 1656, 1587, 1491, 1409 ($C{=}C_{Aromatic}$), 1387, 1363, 1236, 1186 (C-N), 806, 786, 745, 717 ($CH_{Aromatic}$). MS (APCI$^+$, 20 V), m/z: 630 ([M+H]$^+$). Elemental analysis calcd (%) for $C_{43}H_{52}N_2O_2$: C, 82.12; H, 8.33; N, 4.45; O, 5.09. Found: C, 82.17; H, 8.38; N, 4.47.

Instrumentations

^{1}H (300 MHz) and ^{13}C (75 MHz) NMR spectra were recorded on a Varian Unity Inova 300 apparatus at ambient temperature; spectra were analysed with the MestreNova program package. Infrared (IR), melting points, thermogravimetric analysis, differential scanning calorimetry (DSC) measurements, were carried out as described earlier [4]. Mass spectra were recorded on a Waters ZQ 2000 analytical system. Elemental analysis was performed with an Exeter Analytical CE-440 Elemental Analyzer. Theoretical calculations had been carried out with Gaussian 16 and Gaussview 6 softwares.

Absorption, photoluminescence (PL) spectra of dilute solutions and of the films were recorded as described previously. To record PL and phosphorescence spectra as well as PL decays at different temperatures, variable temperature liquid nitrogen cryostat (Optistat DN2) was used. To record the dependencies of delayed emission intensity on laser flux of the samples, the Edinburgh Instruments FLS980 spectrometer and a PicoQuantLDH-D-C-375 laser (wavelength 374 nm) were utilized. Ionization potential measurements of the solid samples were performed by photoelectron emission method in air.

Ionization potentials (IP_{PE}) of compounds in solid-state were investigated by electron photoemission spectroscopy in air. Fluorine doped tin oxide (FTO) coated glass slides were applied as substrates for the preparation of samples for photoelectron emission spectrometry. The layers of the compounds were vacuum deposited onto the substrates. Photoelectron emission spectra were measured in the air using ASBN-D130-CM deep UV deuterium light source, CM110 1/8 m monochromator and Keithley 6517B electrometer/high resistance meter.

Electron and hole mobilities (μ_e, μ_h) were studied by time of flight technique. Samples for TOF measurements were prepared by physical vapor deposition method onto indium-tin-oxide substrates as one of the electrodes.

OLEDs were fabricated by vacuum deposition of organic layers onto cleaned ITO coated glass, vacuum of below 10^{-6} Barr was used. The active area of the obtained devices was 2×3 mm^2, furthermore measurement was made after the device fabrications, in the air without passivation. The first step of the OLED device fabrication process was cleaning ITO substrates by detergent, acetone and deionized water in the ultrasonic bath, respectively and after that whole substrates UV-ozone treated for 30 min. All of the layers related to the fabricated devices were vacuum evaporated at vacuum pressure exceeding 2×10^{-6} mbar. Tests of EL properties were provided immediately after the fabrication of OLEDs in the air without passivation and out-coupling. The current density-voltage and luminance-voltage characteristics were investigated using a sourcemeter Keithley 2400C and calibrated photodiode PH100-Si-HA-D0 together with the PC-Based power and energy monitor 11S-LINK. EL spectra were recorded with an UV-visible Avante spectrometer and CIE coordinates were calculated by using EL spectra. Device efficiencies were calculated using the recorded EL spectra, current density-voltage and luminance-voltage characteristics.

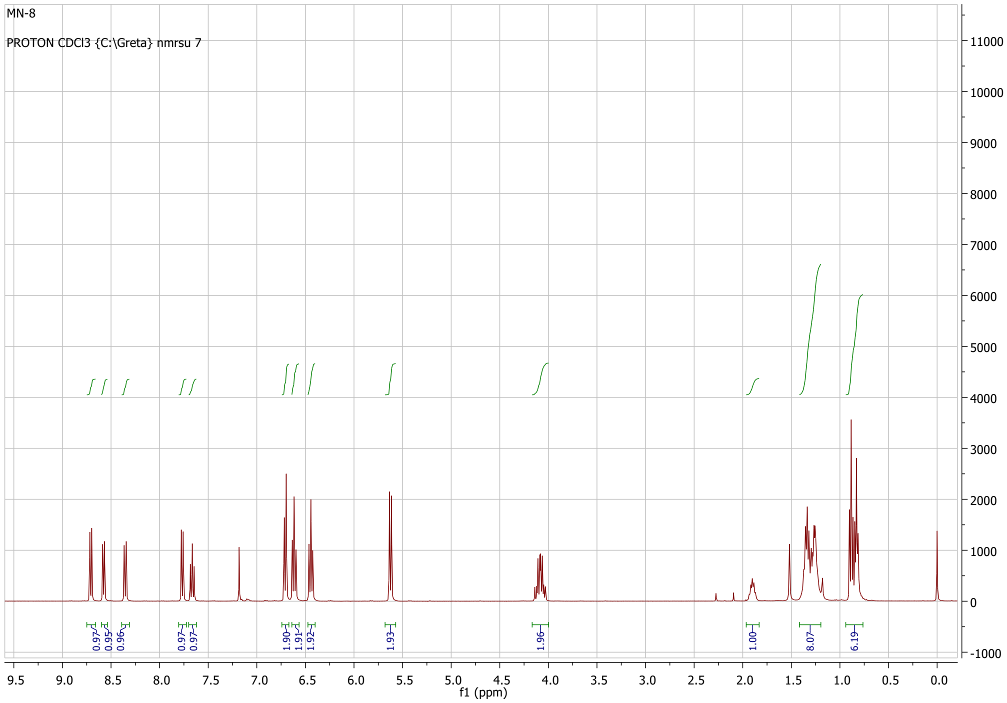

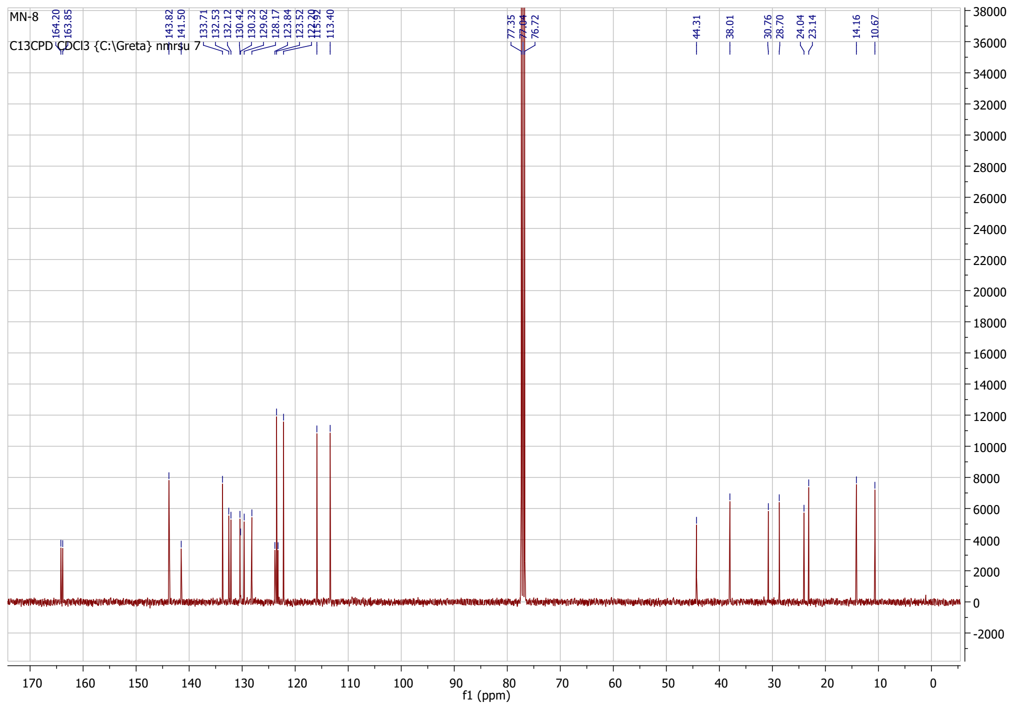

Figure S1. ^{1}H and ^{13}C NMR spectra of cpmpounds **1.**

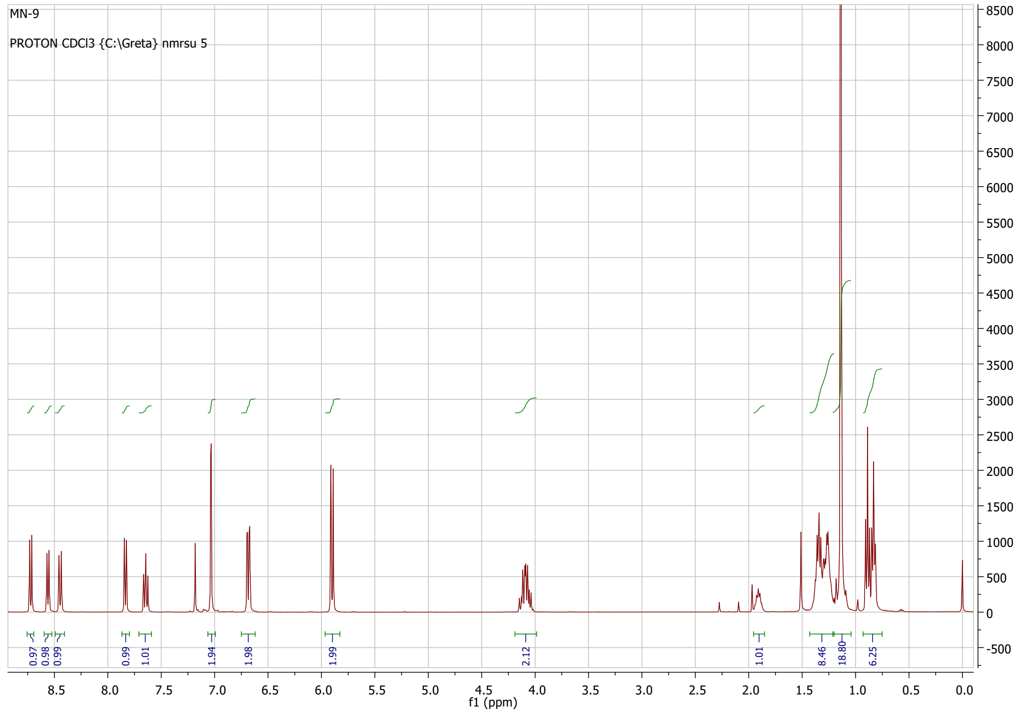

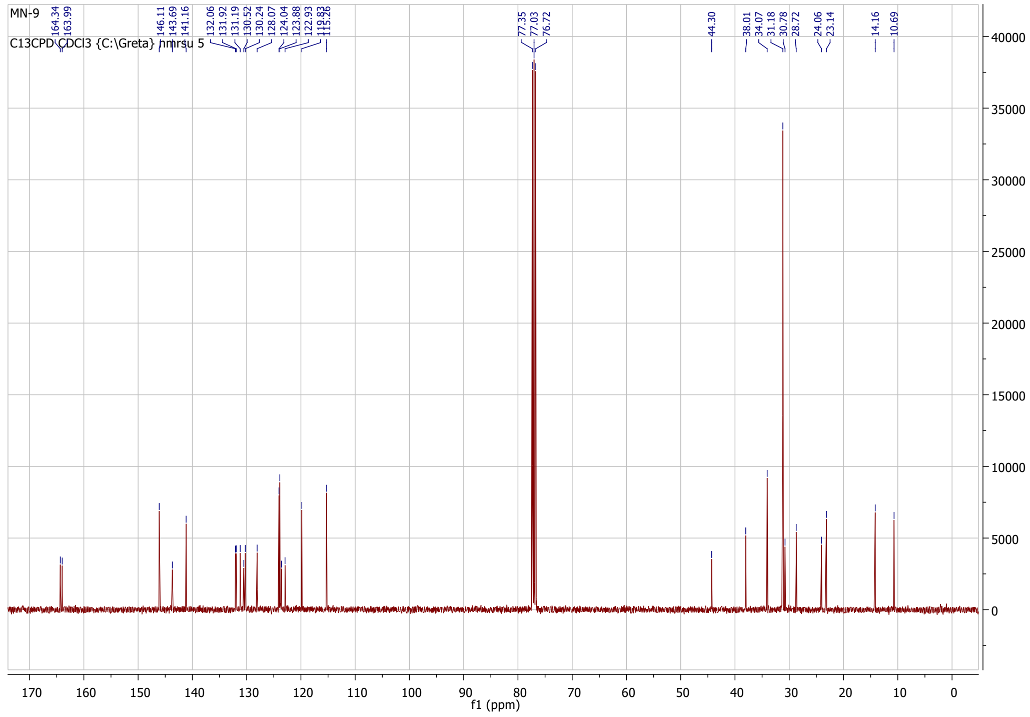

Figure S2. ^{1}H and ^{13}C NMR spectra of cpmpounds **2.**

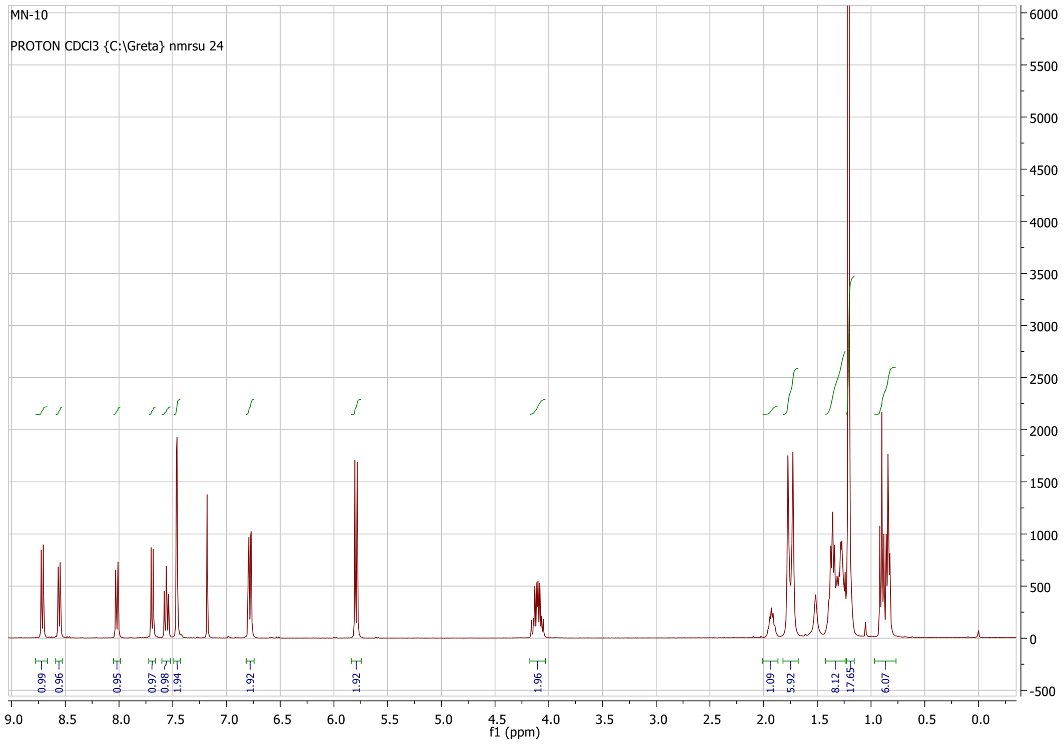

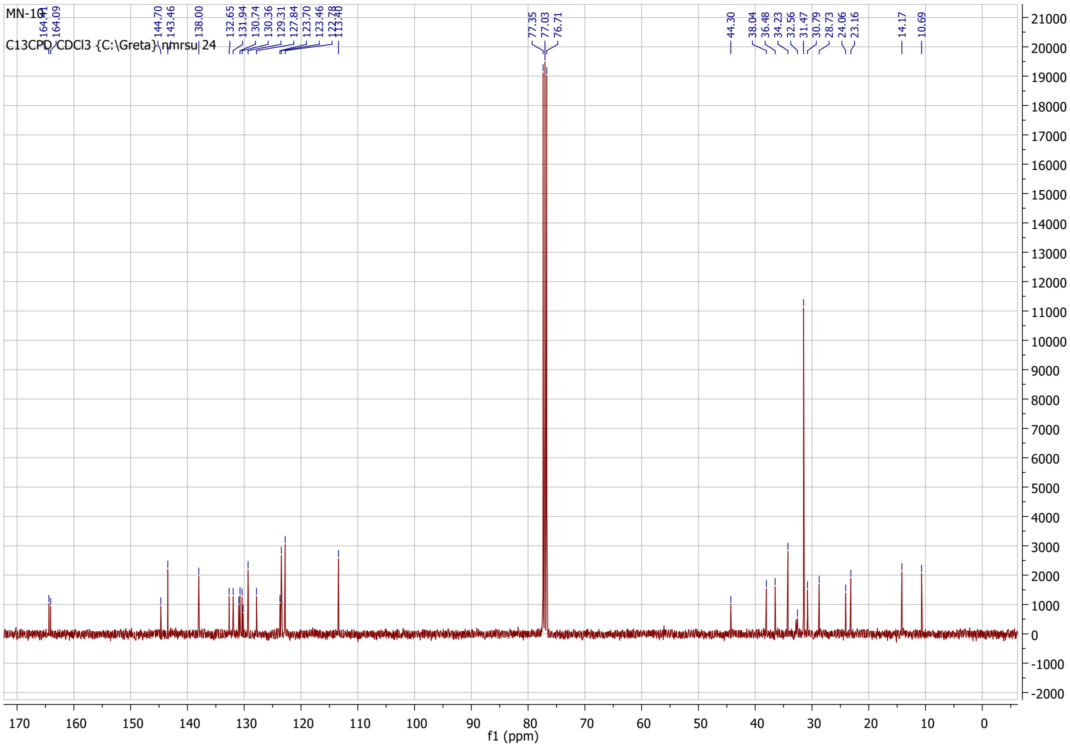

Figure S3. ^{1}H and ^{13}C NMR spectra of cpmpounds **3.**

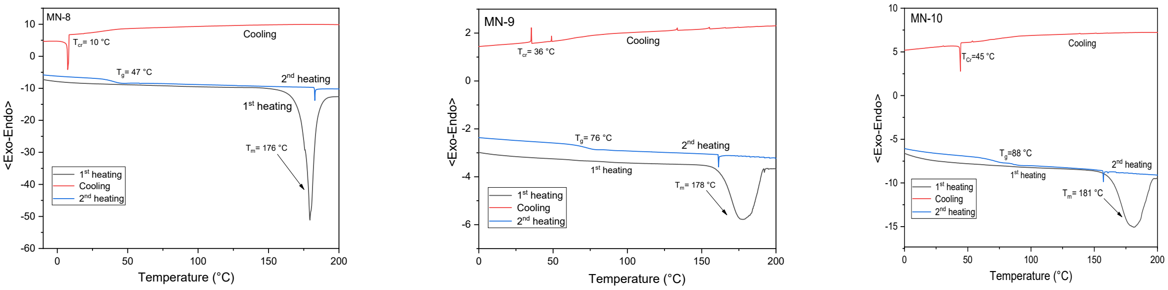

Figure S4. DSC curves of compounds **1-3.**

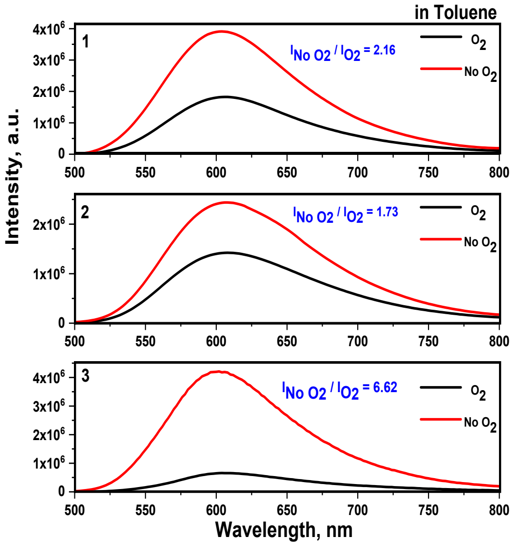

Figure S5. PL spectra of as-prepared and deoxygenated toluene solutions of compounds **1-3**.

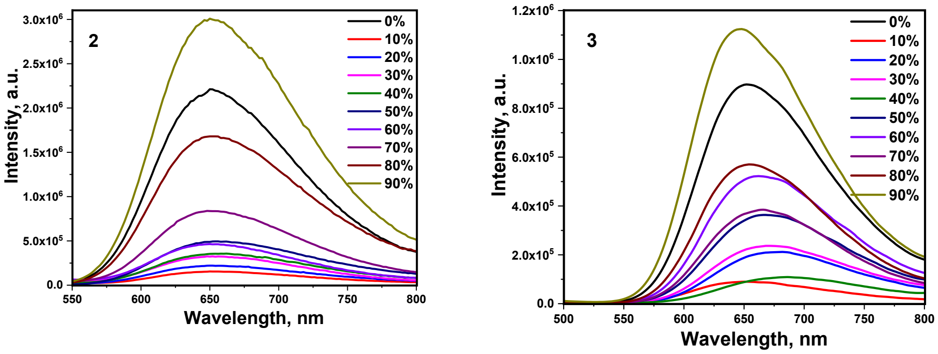

Figure S6. PL spectra of compounds **2** and **3** in THF/water mixtures with different water fractions.

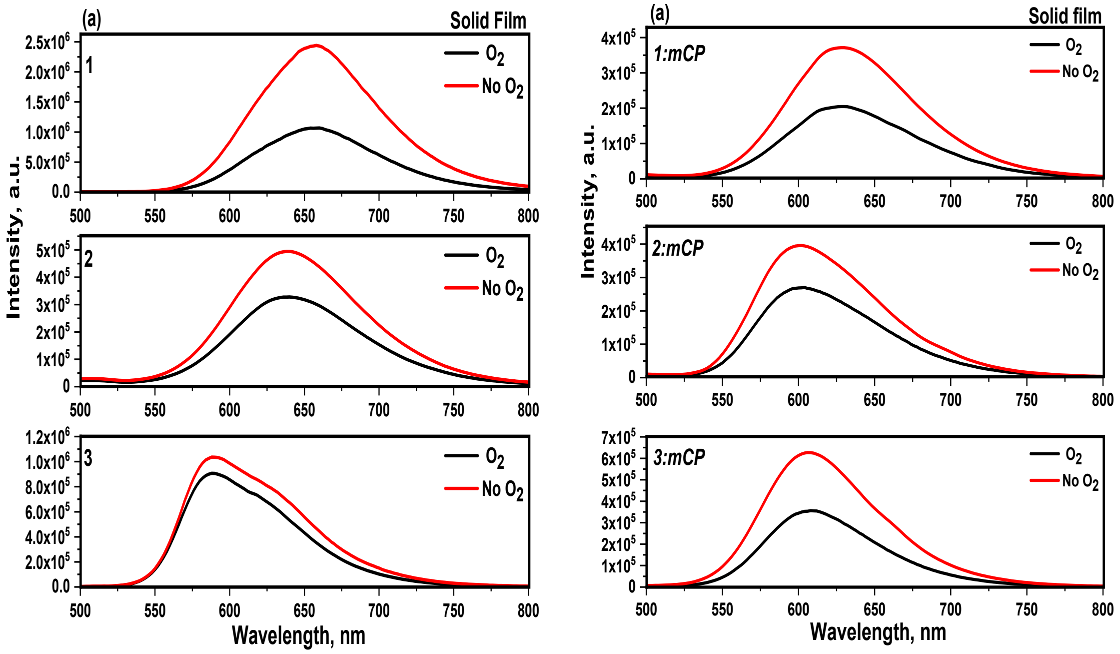

Figure S7. PL spectra of non-doped and doped films of compounds **1-3** under air and vacuum.

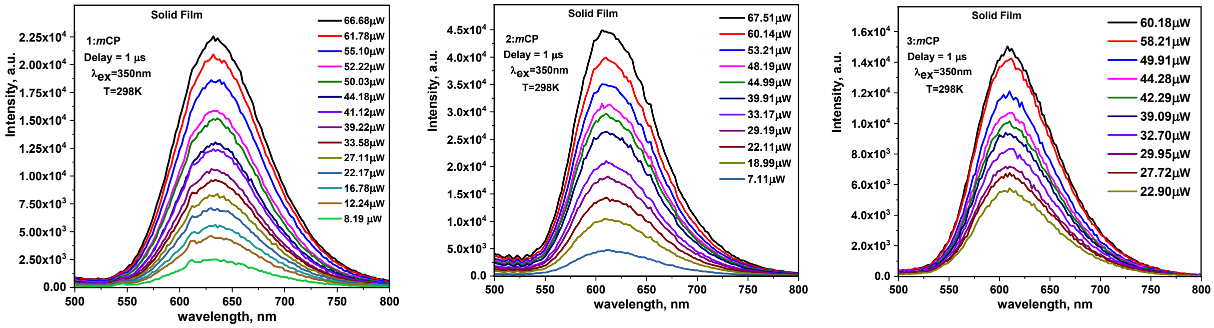

Figure S8. PL spectra of doped film of compounds **1-3** at the different power of excitation.

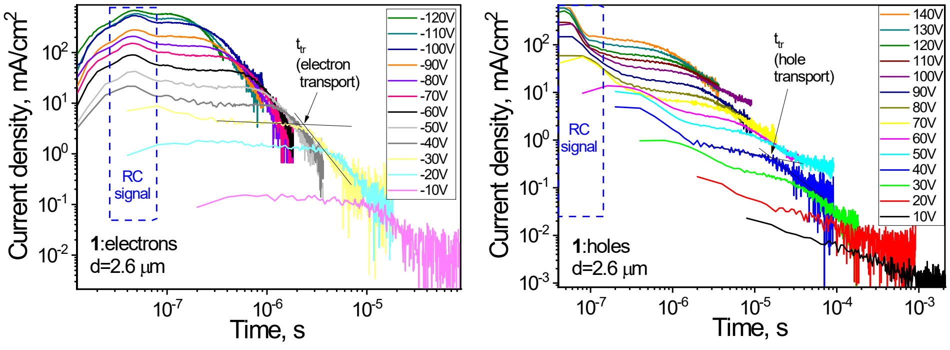

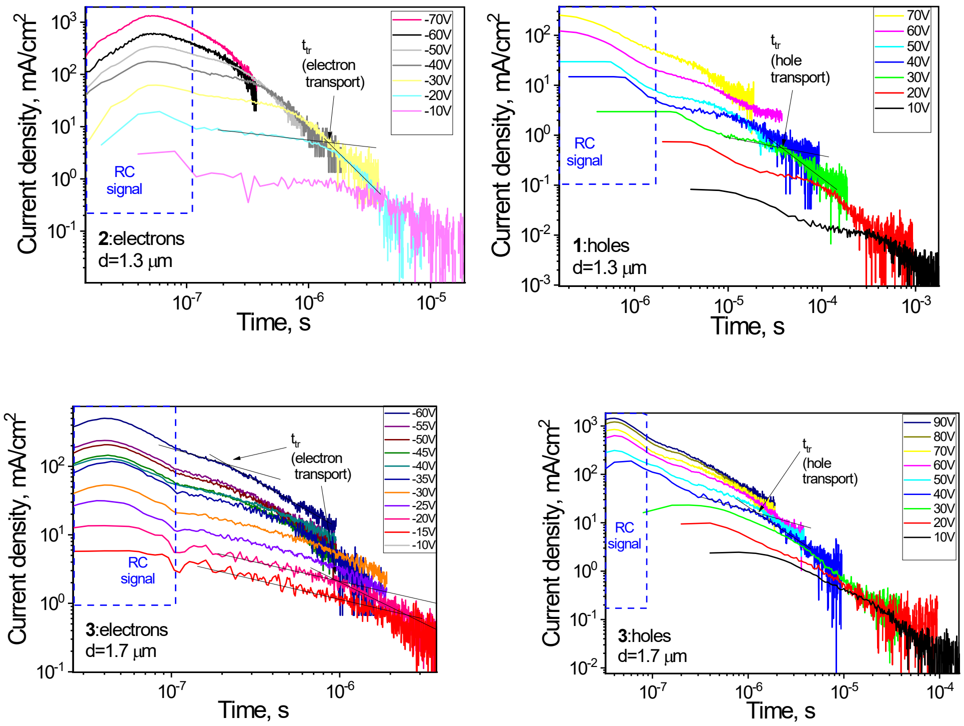

Figure S9. TOF transients for electrons (b) and holes (c) in film of compounds **1-3** at different applied voltages/electric fields.

Table S1. Comparison of reprecentive paramiters of TADF OLED emitters based on 1,8-naphthalimide moiety.

Number	Structure	PLQY (%) Film	EQE (%)	Non-doped or Doped OLED	Ref.
1	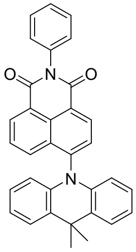	21.5	11.2	Doped: *m*CPPFP:emitter	[5]
2	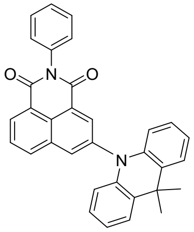	5.2	4.6	Doped: *m*CPPFP:emitter	

3	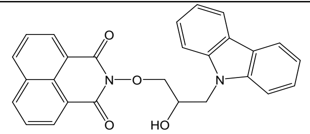	6.0±2	1.02	Non-doped	[6]
4	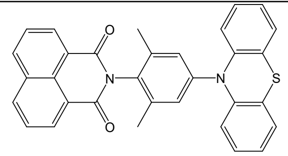	55	7.13	Doped: emitter CBP: emitter	[7]
5	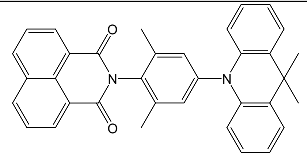	39	5.38	Doped: emitter CBP: emitter	
6	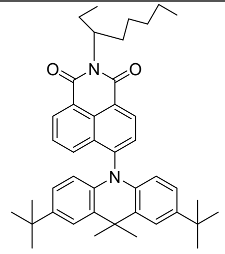	77	8.2	Doped: *m*CP:emitter	This study

List of references

[1] Gudeika D, Michaleviciute A, Grazulevicius J V., Lygaitis R, Grigalevicius S, Jankauskas V, et al. Structure properties relationship of donor-acceptor derivatives of triphenylamine and 1,8-naphthalimide. J Phys Chem C 2012;116. https://doi.org/10.1021/jp303172b.

[2] Kormos CM, Leadbeater NE. Direct conversion of aryl halides to phenols using high-temperature or near-critical water and microwave heating. Tetrahedron 2006;62. https://doi.org/10.1016/j.tet.2006.01.103.

[3] Yofu K, Nomura K, Fukuzaki E, Hirai Y, Hamano M, Mitsui T. Photoelectric conversion material, film containing the material, photoelectric conversion device, method for preparing photoelectric conversion device, method for using photoelectric conversion device, photosensor and imaging device. US9349965, 2016.

[4] Gudeika D, Volyniuk D, Mimaite V, Lytvyn R, Butkute R, Bezvikonnyi O, et al. Carbazolyl-substituted quinazolinones as high-triplet-energy materials for phosphorescent organic light emitting diodes. Dye Pigment 2017;142. https://doi.org/10.1016/j.dyepig.2017.03.066.

[5] Yun JH, Lee JY. Benzoisoquinoline-1,3-dione acceptor based red thermally activated delayed fluorescent emitters. Dye Pigment 2017;144. https://doi.org/10.1016/j.dyepig.2017.05.036.

[6] Bezuglyi M, Ivaniuk K, Volyniuk D, Gražulevičius J V., Bagdžiūnas G. An approach to discovering novel exciplex supramolecular complex based on carbazole-containing 1,8-naphthalimide. Dye Pigment 2018;149. https://doi.org/10.1016/j.dyepig.2017.10.013.

[7] Wu Y, Chen X, Mu Y, Yang Z, Mao Z, Zhao J, et al. Two thermally stable and AIE active 1,8-naphthalimide derivatives with red efficient thermally activated delayed fluorescence. Dye Pigment 2019;169. https://doi.org/10.1016/j.dyepig.2019.04.071.